Characterization of thermo-rheological behavior of polymer melts during the micro injection molding process

N Zhang[1] and *M D Gilchrist[1]

[1]School of Mechanical and Materials Engineering, University College Dublin, Ireland

*Corresponding Author: michael.gilchrist@ucd.ie

Abstract: In-line process monitoring and rheological characterization can help to understand the behavior of polymer melt flows during manufacturing and to make injection molding a measurable process for manufacturing high quality parts. This work developed an in-line rheology measurement system using a slit die attached to a micro injection molding machine. A series of dog-bone mold inserts was used to form the slit die with thickness ranging from 600μm to 200μm. Two combined pressure and temperature sensors were embedded into the slit die to measure the pressure drop. Based on the slit flow model, it was found that the viscosity of Pebax melts depends on the slit thickness in the actual injection molding process. The competing effects of wall slip and non-isothermal conditions will determine the melt viscosity. The plastication induced thermo-mechanical history can also influence polymer viscosity, although it is neglected in conventional rheology measurements.

Keywords: Rheology, Micro injection molding, Slit die, Non-isothermal process, Pebax

1. Introduction

Rheological characterization of polymer melts is widely used in process monitoring, quality control, process design and simulation, and troubleshooting applications [1]. Generally, instrumentation based on rotational, capillary or slit flows used to obtain accurate measurements at a series of set strain rates and temperatures [2]. Some work has been done by using slit/capillary dies embedded into either nozzles or molds to test the material rheology with an injection molding machine or an extruder [1-6]. This method can provide rheological data associated with the same thermo-mechanical history that is experienced by materials during real process conditions, such as plastication and viscous heating.

Based on conventional injection molding technology, micro injection molding has demonstrated itself to be the most efficient way to fabricate polymer micro components with complex shapes and products with high quality surface features [7]. However, both micro parts and micro/nano features have very high surface to volume ratios, making heat diffusion effects very significant. As a result, the polymer melt solidifies even faster. The elevated temperature and higher pressure are mainly used to fill the polymer melt into micro cavities as quickly as possible. Consequently, the polymer melt will experience very high shear rates and very high thermal gradients in the micro injection molding process. Melt rheology under such extreme conditions controls the polymer flow behavior at the micro/nano meter scale. Based on numerical simulations, Yao et al. [8] studied the effect of size related viscosity, wall slip and surface tension on the filling of micro channels and found that micro viscosity and wall slip must be considered when channel size is smaller than 10μm. They also found that surface tension is not important for micro injection molding. They also found that viscous heating is not significant when channel size is smaller than 100 μm. Kelly et al. [2] used an embedded capillary die instead of a nozzle to obtain an extremely high shear rate viscosity. They found when the shear rates approached or exceeded 10^{-6} 1/s, that viscosity reached a rate independent plateau, and in some cases shear thickening happened with further increases in shear rate. This was attributed to molecular structure. Chien et al. [9] developed a series of micro-channels in a die that was embedded in a mold in order to study the rheological behavior of polymer melts under isothermal conditions using an injection molding machine. They found that the viscosity of polymer melts in the micro-channels is significantly lower than that measured when using a conventional capillary rheometer. They also found that wall slip velocity increases with decreasing micro-channel size and that there is a large reduction in apparent viscosity when the size of a micro-channel decreases. Similar work by Vasco et al. [10] on the thermo-rheological behavior of polymer melts in micro channels, when mold temperature is lower than melt temperature, indicates that a heat transfer analysis of conventional injection molding is not applicable to a very thin micro injection molding with a very large surface to volume ratio. Although

these studies give some insight into the polymer rheology behavior at the micrometer scale, they either focused on viscosity measurement under assumed isothermal conditions or they did not separate the effects of plastication, wall slip and non-isothermal conditions when analysing rheological behavior.

In the present work, the rheological behavior of polymer melts was measured with several adjustable dog-bone slit dies with thicknesses ranging from 600μm to 200μm using a commercial micro injection molding machine and a process monitoring system. By recording the pressure drop and cross-section of the gage length of the dog-bone parts, viscosity was calculated according to the slit flow model. By varying the machine process parameters, the dependence of viscosity on slit thickness was quantified along with the effects of plastication on viscosity. Based on a dimensionless analysis and the power-law slip model, it was possible to establish the influence of non-isothermal processes, slit thickness and wall slip on viscosity.

2. Flow model

2.1 Slit flow model

A slit is defined as a straight, rectangular channel having width, w, which is much greater than its thickness, h. The effect of edges on pressure drop is ignored. In the measurement, the polymer melt is forced by a piston to flow though a slit die, as shown in Fig. 1. With the assumptions of a fully developed steady state laminar flow with no-slip on the wall, viscosity can be calculated by monitoring the amount of polymer exiting the slit die per unit time (Q) for a given pressure drop (ΔP)[11].

Fig. 1.

The apparent shear rate and real shear stress in the slit model are given by

$$\dot{\gamma}_{w(app)} = \frac{6Q}{wh^2} \tag{1}$$

and

$$\tau_{w(real)} = \frac{h}{2}\left(\frac{-\Delta P}{L}\right) \tag{2}$$

where L is length, as shown in Fig. 1. When the ratio of w/h of a rectangular channel is less than 10, the edge effect on the shear stress must be corrected. The wall shear stress for Newtonian fluids is given by [13]

$$\tau_{w(real)} = \frac{w \cdot h}{2(w+h)}\left(\frac{-\Delta P}{L}\right) \tag{3}$$

According to the Walter correction [14], the wall shear rate of a non-Newtonian fluid can be determined by

$$\dot{\gamma}_{w(real)} = \frac{6Q}{w \cdot h^2}\left(\frac{2}{3}+\frac{1}{3}n\right) \tag{4}$$

where n (power law index) is the slope of $\log \dot{\gamma}_{w(app)}$ versus $\log \tau_w$. The disadvantage of Eq. 4 for in-line rheological measurements is that n is unknown. In order to obtain one point of the true viscosity function from each single measurement of τ_w and $\dot{\gamma}_{w(app)}$, a modified correction associated with the concept of a representative viscosity was introduced by Schümmer and co-workers [15] and was used in this work, taking the non-Newtonian velocity into account. They proposed an approximation procedure based on estimating the shear rate and viscosity at a vertical distance y_s where the apparent shear rate equals the true shear rate. At this point, the shear stress and the apparent shear rate, respectively, take the values $x^*\tau$ and $x^*\dot{\gamma}_{w(app)}$, where $x^* = 2y_s/h$. Therefore,

$$\eta(x^*\dot{\gamma}_{w(app)}) = \eta_a(\dot{\gamma}_{w(app)}) = \frac{x^*\tau}{x^*\dot{\gamma}_{w(app)}} \tag{5}$$

For a power-law fluid and capillary flow, it can be shown that

$$x^* = \left(\frac{3n+1}{4n}\right)^{n/(n-1)} \tag{6}$$

X^* is a weak function of n, which is 0.79 for a slit geometry [13]. Thus, it is possible to calculate the viscosity at one shear rate using data from a single experiment or to shift the entire apparent viscosity data horizontally to obtain the real viscosity.

2.2 Wall slip

Generally speaking, viscous fluids adhere to and attain the velocity of the boundry during flow. However, a relative velocity exists at the contact line between the fluid and solid boundary during flow: this is the so called "wall slip" [16]. Slip of polymer melts is explained by flow induced chain detachment/desorption and chain disentanglement. According to Hatzikiriakos & Dealy's experiments with sliding plate and capillary rheometers [17, 18], wall slip occurs when the shear stress exceeds a critical stress, which is around 0.1MPa for Polyethylene. The various experimental methods of determining wall slip velocity can be found in an excellent review by Hatzikiriakos [19]. Classic gap-dependence methods, such as Mooney's method [20] and the sliding plate rheometer [17], need a series of capillaries/slits with different diameters or thicknesses. Flow visualization with optical techniques involves additional equipment, such as tracing particles and specially designed monitoring systems. Rosenbaum & Hatzikiriakos [21] used a simple modified power-law expression without pressure or temperature dependence to estimate the slip velocity

$$u_s = \frac{a}{1+(\tau_c/\tau_w)^{10}}\tau_w^m \tag{7}$$

where τ_w is wall shear stress, τ_c is wall critical stress, a is the temperature dependent slip coefficient and m is a power law index (~3 for Polyethylene). This model has been used by Yao and Kim [8] in their numerical simulation of the filling of micro scale channels and by Vasco et al. [10] to predict the slip velocity when polymer melts fill though 200μm×200μm and 400μm×100μm channels.

3. Experiment Methods

3.1 Rheology monitoring system

The viscosity of polymer melts was measured with an insert mold utilising a reciprocating micro injection molding machine, Fanuc Roboshot S-2000i 15B, which was equipped with a 14mm diameter injection screw. We designed a series of adjustable dog-bone mold cavity inserts to form the mold cavities with depths of 600, 500, 400, 300 and 200 μm, as shown in Fig. 2 (a) and (b). Steel and bulk metallic glass (BMG) were used as mold insert materials, as shown in Fig. 2 (c). Pebax 7233 (Arkema Group) was used as the molding material. The raw material pellets were dried in a vacuum chamber at 65^{o}C for 4 hours before use. Figure 2 (d) displays the molded part, which weighed around 31mg (thickness ~500μm). The combined volume of the sprue, runner and gate was 289 mm^3, which was around 11.5 times the volume of the 0.5mm thick dog-bone part (25mm^3). Two Kistler 6189A combined pressure and temperature sensors (PT sensors) with tip diameters of 2.5mm were fitted into the waisted region of the dog-bone mold cavity to directly detect the melt temperature and cavity pressure at the same position, as shown in Fig. 3 (a). A Kistler CoMo injection process monitoring system (2869B) was used for data acquisition (Fig. 3 (b)). The cavity pressure and material contact temperature were initially collected by the CoMo and then were outputted into a computer by Ethernet. Moreover, the injection velocity, injection pressure and screw position during the injection molding process were also outputted into the CoMo system. The injection signals from the injection molding machine triggered the CoMo to ensure that all signals were received simultaneously.

Fig. 2.

Fig. 3.

3.2 Process parameter settings

Typical injection velocities from 10mm/s to 300mm/s were selected to realise the wide range of shear rates. Trial and error was used to find the process parameters that ensured all thickness parts were fully filled, as shown in Table 1. The melt and mold temperatures were set below the melting temperature of Pebax and varied in three levels.

Three important factors during plastication, namely back pressure, screw rotation speed and dwell time, were also set in three levels to characterize the effect of plastication on melt rheological behaviour. The shot size of all the process conditions was set as 12mm. Each of the settings was repeated 10 times and five consecutive cycles were randomly selected to calculate the viscosity of polymer melts during the micro injection molding process.

3.3 Pressure drop

Generally, the conventional slit rheometer is a rectangular slit and the pressure drop can be directly recorded without any end correction. In the present work, however, the cavity was designed to be dog-bone in shape (c.f. Fig. 4.) so that the molded parts could be used for mechanical testing. Moreover, the relatively larger PT sensor tips could be fitted into the mold cavity. As the result, the waisted regions could have influenced the pressure drop along the gage length. However, for most commercial thermoplastic polymers, when the ratio of capillary length to diameter is over 20, the Bagley end correction can be ignored except for very high molecular weight polymers [22]. For our case, the ratios of length to depth vary from 20-50 except for the 600μm cavity thickness for which the ratio is 16. Therefore, we believe that the entrance and exit waist regions would actually have a negligible effect on pressure drop. The pressure gradient can be approximated by $\Delta P_{total}/\Delta L_{total}$, as shown in Fig. 4. As the total pressure drop can be recorded by PT sensors, the gage region of length L and of width W were used to calculate the apparent viscosity.

Figure 5 shows the typical trace curves of cavity pressure during 0.08s. It can be observed that the melt front reaches sensor 1 near the gate and travels to sensor 2 during time Δt_1 and the pressure drop is uniform during Δt_2 when the melt front reaches the end of the part. The average pressure drop during Δt_2 was used to calculate the pressure gradient.

Table 1

Fig. 4.

Fig. 5.

3.4 Volume flow rate

For a conventional rheometer, the slit/capillary die is connected to a barrel equipped with a piston to form the melt delivery system, as shown in Fig. 1. The volume flow rate is obtained from the measured piston speed, V_P, and the piston cross-sectional area, $Q=A_PV_P$ [2-5]. In the injection molding process, the molten polymer is injected by the injection screw though the injection nozzle, sprue, runner and gate into the cavity, as shown in Fig. 3 (a). For the current system, the volume of polymer melt injected under the preset injection stroke made by the injection screw can be calculated from the screw position recorded by the CoMo process monitoring system, as shown in Fig. 5. The theoretical injection volume can be calculated by $V_L=\pi D^2S/4$, where V_L is the theoretical injection volume (mm^3), D is the screw diameter (mm); S is the actual injection stroke of the injection screw (mm). However, for micro injection molding, the volume of the micro component is even smaller than the unit metering volume of the machine. As a result, volume variations from the material PVT behavior and leakage flow due to delays of the check ring shutting off is even greater than the volume flow into the cavity. Moreover, the high injection pressure that is associated with filling micro cavities makes the melt density vary more significantly. Figure 6 shows the comparison of the theoretical volume calculated from the screw displacement and air shot volume under the same process conditions. Ignoring the effect of pressure and temperature on volume, the actual injection volume is around 78% of the theoretical injection volume under different injection velocities. In addition, as indicated in Fig. 7, the injection molding machine can only maintain the set injection velocity at low values and not at high values, such as 300mm/s. Therefore, it is inproper to use injection velocity to calculate the volume flow rate in the same way as would be done for conventional injection molding. Instead, the actual volume flow rate can be calculated by the actual volume of the dog-bone part between sensor 1 and sensor 2 over the time the melts travels this corresponding distance (Δt_1).

Fig. 6.

Fig. 7.

4. Results and discussion

4.1 Conventional rheological behavior of polymer melts

The rheological data of Pebax 7233 at temperatures of 200°C, 230°C and 260°C as provided by the material supplier is shown in Fig. 8 [23]. Pebax is a thermo-rheologically simple polymer and its viscosity-temperature relationship can be described by the Arrhenius equation,

$$\eta(T) = A \cdot \exp\left(\frac{E}{RT}\right) \tag{7}$$

where A is a resin dependent constant, T is melt temperature, R is the gas constant and E is the flow activation energy. Based on data fitting at high shear rates (>1000 1/s), the flow activation energy is approximately 25.9 kJ mol^{-1}.

According to the time-temperature superposition principle, a dimensionless temperature shift factor a_T can be determined by

$$a_T = \exp\left(\frac{E}{R}\left(\frac{1}{T} - \frac{1}{T_{ref}}\right)\right) \tag{8}$$

where $R=8.314*10^{-3}kJ/(mol\ K)$, T_{ref} is a reference temperature and T is the objective temperature. The objective temperature was set at 210°C, which equals the melt temperature in the current experiments. Data fitting gives the different a_T when shifted to 210°C: 0.87 (T_{ref}=200°C), 1.29 (T_{ref}=230°C) and 1.83 (T_{ref}=260°C). All the viscosity data under different temperatures were shifted to 210°C, as shown in Fig. 9. It can be seen that the data fitting is particularly good at high shear rates.

Fig. 8.

Fig. 9

The Carreau-Yasuda viscosity function was used to describe the rheological behavior. Viscosity data shifted from 200°C was used to fit the viscosity model,

$$\eta(\dot{\gamma}) = \eta_0\left[1 + (\lambda\dot{\gamma})^a\right]^{(m-1)/a} \tag{9}$$

where η_0 is the zero shear rate viscosity, λ is a characteristic time, m is the power law exponent and a is a transition width parameter. Figure 10 shows the data fit with the Carreau-Yasuda model and the parameters of this model are shown in Table 2.

Fig. 10.

Table 2

4.2 Micro cavity flow

4.2.1Viscosity with different slit thicknesses

Based on the slit flow model and the Schümmer correction, the apparent and actual viscosities of Pebax under real micro injection molding conditions can be obtained. The comparison between the Carreau-Yasuda viscosity model and the micro dog-bone slit viscosity is shown in Fig. 11. Four important features can be found: the measured viscosity is well below the conventionally predicted viscosity; the viscosity of polymer melt depends on the slit thickness; viscosity decreases as the slit thickness increases and the measured viscosities of the 400μm, 500μm and 600μm cavities are almost identical; the viscosity curves converge as the shear rate increases. As shown in Fig. 12, the viscosity deceases as melt temperature and mold temperature increase. In addition, we also manufactured a BMG slit and a steel slit with the same thickness of 300μm. As shown in Fig. 13, the viscosities measured using both the BMG and steel are identical, which indicates that there is no significant difference between BMG and steel on rheological behavior.

During conventional rheological measurements, the melt flow is kept under isothermal conditions to eliminate any effects of heat diffusion on viscosity. However, in an actual injection molding process, the mold temperature is set well below the melt temperature in order to cool the part. This makes filling a non-isothermal process. For micro injection molding, due to the high surface to volume ratio, the heat diffusion is even more significant and will

influence the monitored viscosity. Therefore, the non-isothermal flow needs to be taken into account when explaining the slit thickness dependent viscosity.

Fig. 11.

Fig. 12.

Fig. 13.

4.2.2 Non-isothermal flow

The energy balance in vector-tensor form is given by the following equation [24]:

$$\rho c_p\left(\frac{\partial T}{\partial t}+\underline{v}\cdot\nabla T\right)=k\nabla\cdot\nabla T+\frac{1}{2}\dot{\underline{\underline{\gamma}}} \tag{10}$$

There are four contributions in this energy equation: (i) heat conduction in the flow direction, (ii) heat conduction in the thickness direction, (iii) heat convection in the flow direction, (iv) viscous heating. Yao and Kim [24] used several dimensionless numbers to analysis the relative importance of sources for energy balance. These dimensionless numbers were also used to characterize the current dog-bone slit cavity.

Peclet Number (Pe) is the ratio of heat conduction to heat convection along the flow direction, defined as

$$Pe=\frac{uL}{\alpha} \tag{11}$$

where u is averge filling velocity, L is length of slit cavity (L= 9.77mm) and thermal diffusivity $\alpha\sim10^{-7}m^2/s$.

Graetz Number (Gz) is the ratio of heat convection in one direction to heat conduction in another direction. It also can be understood as the ratio of the time required for heat conducting from the center of a cavity to the mold wall to the average residence time in the cavity. For the present cavity, the main heat conduction is in the thickness direction and major convection is in the flow direction. Therefore,

$$Gz=\frac{uh^2}{\alpha L} \tag{12}$$

Brinkman Number is the ratio of viscous heating to heat conduction from an imposed temeprature difference. It can be represented by

$$Br=\frac{\eta u^2}{k\Delta T} \tag{13}$$

Because $Q=uA$, when substituted into Eq.1, the average velocity u can be expressed as a function of the apparent shear rate $\dot{\gamma}_{w(app)}$,

$$u=\frac{\dot{\gamma}_{w(app)}\cdot h}{6} \tag{14}$$

Substituting Eq.13 into the dimensionless groups, the relationship of Pe, Gz and Br on shear rate and cavity thickness can be found, where k=0.23W/m^{o}C and $\Delta T=T_{melt}-T_{wall}$=90^{o}C

As shown in Fig. 14, Pe ,Gz and Br are thickness and shear rate dependent. They both increase with the increase of shear rate and cavity thickness. In addition, they converge with a decreasing shear rate. For Pe, it indicates that heat conduction along the flow direction becomes more important for thin slits at lower filling velocities. However, when shear rate reaches its lowest values ($3\times10^3$1/s), Pe is still ~2×10^4. Thererfore, heat conduction along the flow direction can be safely neglected. Gz reduces to 10 when the shear rate reaches these lowest values ($3\times10^3$1/s); this indicates that heat convection along the flow direction is more important than transverse heat conduction. Br varies from 0.2 to 9 over the range of shear rates and cavity thicknesses. When Br≥1, viscous heating would have a more signficant effect than heat conduction. Viscous heating increases with shear rate and cavity thickness, although it has less effect at lower filling velocities for relatively thinner cavities.

Fig. 14.

4.2.3 Wall slip

Generally, the wall shear stress increases with shear rate for a non-slip wall-polymer interface. The onset of slip is determined by a critical shear stress. According to experimental observations [25], there are three slip regimes: (i) a weak slip regime at low shear stresses when slip exceeds a first critical stress σ_{c1} (0.1~0.3MPa) and the shear stress–shear rate relationship first becomes nonlinear due to adhesive failure from flow induced polymer chain detachment; (ii) a stick-slip regime at intermediate shear stresses marked by periodic oscillations in slip velocity and shear stress; (iii) a strong slip regime at high shear stresses. Figure 15 depicts the flow curves of Pebax melts under different cavity thicknesses in the actual micro molding process. For 200μm and 300μm thick slits, the shear stress reduces with increasing shear rates. This indicates that polymer melts might be located in the stick-slip regime and disentanglement of polymer chains induces stress relaxation. On the other hand, for the slits that are at least 400 μm thick, the shear stress gradually increases with shear rate with small slope and the polymer melt might be in the weak slip or stick-slip regime.

Because the slip behavior of Pebax was not characterised, the critical stress τ_c, slip coefficient a and power law index m in Eq. 7 are unknown. Therefore, the relative slip velocity was defined as slip velocity over the maximum slip velocity ($u_s/u_{s(max)}$) in order to describe the slip behaviour for different thickness slit cavities. Assuming the power law index $m=3$ [17], the defined relative slip velocity is shown in Fig. 16. Generally, the relative slip velocity decreases as cavity thickness increases except for a 400μm slit. This can be explained by the flow curves in Fig. 15. It is clear that the shear stresses reduce as the slit thickness increases except for the 400μm thick slit cavity. It was identical to the stress measured from the 600μm slit. This is because the insert forming the 400μm slit was polished to a low average roughness of ~30nm. On the other hand, the inserts forming the 500μm cavity had a high average roughness of ~200nm. This rough surface inhibited the flow of polymers which needed greater force.

Figure 17 illustrates the flow curves under different melt and mold temperatures. The shear stress decreases with melt temperature. Lower mold temperatures can also increase the shear stress, although this is not obvious when mold temperature is lower than 100°C, as indicated by the similarity of the shear stresses at 100°C and 80°C. Figure 18 shows the shear stress when using 300μm thick BMG and steel inserts. Although BMG was polished with an average roughness of ~30nm compared to the relatively rough steel insert, which had a surface roughness of ~200nm, there was no significant difference between the corresponding shear stress. This indicates that the effect of heat transfer might be more important than surface roughness on polymer viscosity for the 300μm thick slit cavity.

Fig. 15.

Fig. 16.

Fig. 17.

Fig. 18.

4.2.4 Interpreting slit thickness dependent viscosity

We start by assuming that the conventional viscosity of a polymer melt is free of slip at the relatively lower shear rates. The viscosity predicted by the Carreau-Yasuda model can be considered as that without slip. It is well know that viscosity decreases with temperature. As discussed in Section 4.2.2, heat convection dominates over heat diffusion during the filling process for all slit cavities. The competing effects of heat transfer and viscous dissipation will determine the actual melt temperature during the filling process. Generally, wall slip can reduce the shear stress needed to force a polymer melt thought the slit cavities and consequently can serve to reduce the viscosity. Experimental work by Chien et al. [9] and simulation by Yao & Kim [24] both confirm that wall slip can significantly reduce the viscosity of polymer melts.

For either the lowest shear rate or the thinnest slit (200 μm), heat conduction dominated the heat transfer and the relatively small amount of viscous dissipation could be neglected. In normal conditions, the measured viscosity should be higher than the non-slip viscosity when mold temperature is set below the melt temperature. However, as seen in Fig. 11, all the measured viscosities were well below those predicted by the Carreau-Yasuda model. This implies that wall slip occurred and significantly reduced the viscosity. In addition, it was also observed that the viscosity generally decreased as slit thickness increased. This could have been because viscous heating induced a temperature increase. Moreover, the frozen surface layer formed quickly due to heat conduction. This served to reduce the slit cross section, especially for thinner slits. As a result, even more pressure was needed to force polymer though the reduced cavity, leading to an increase of shear stress and viscosity. Although the wall slip velocity decreased with slit thickness, the reduced viscosity with slit thickness indicates that viscous heating and the frozen

surface layer may have played a more important role. The measured viscosity for the 400μm, 500μm and 600μm slits were relatively similar, due to their similar shear stresses and wall slip velocities, although the heat transfer conditions were different. The viscosity of the 400 μm slit was smaller than that of the 500μm slit. This is because the lower surface roughness served to reduce the shear stress. The viscosity values converged at increasing shear rates and this trend is similar to the slip velocity and is contrary to Pe, Gz and Br. This means that, overall, it is wall slip that governs the viscosity.

4.3 Effect of plastication on viscosity

The rheological characterization of polymer melts for injection molding is commonly carried out using a capillary rheometer with raw polymer material, neglecting the influence of the plastication phase. Bariani et al.[4] compared the viscosity measured by a twin bore capillary rheometer and an in-line slit rheometer using an injection molding machine. The viscosities were similar when measured by both methods. This means that the thermomechanical history from the plastication phase does not have a significant effect on the rheological behavior of polymer melts for conventional injection molding.

We used our current system to study this for the micro injection molding process. As shown in Table 1, three important parameters of the plastication stage were selected: back pressure, screw rotation speed and dwell time. A 500μm slit was used with a melt temperature of 210^{o}C and mold temperature of 120^{o}C. As shown in Fig. 19, all selected parameters had some influence on viscosity. The viscosity decreased at increasing back pressure because of the increasing friction induced heat during screw rotation. When screw rotation speed was lower than 100rpm, there was no change in viscosity. When rotation speed reached 150rpm, the viscosity increased. This could have been because the faster rotation caused slippage of the material and the temperature levelled off or even decreased. The dwell time had less of an effect on viscosity although longer dwell times did cause a small reduction in viscosity. However, for heat sensitive polymers, too long a dwell time could cause material degradation.

Fig. 19.

5. Conclusions

In the present work, a measurement system to quantitatively evaluate the rheological behavior of polymer melts under a typical micro injection molding process was established. The flow curves of a slit dog-bone cavity with thicknesses ranging from 600μm to 200μm were monitored. Three dimensionless numbers, Pe, Gz and Br, were used to evaluate the non-isothermal process that the material experienced during the actual molding process. Four important observations can be made about the viscosity of polymer melts in the actual micro injection molding process:

- The measured viscosity is well below the predicted conventional viscosity;
- The viscosity of polymer melts depends on the slit thickness;
- The viscosity decreases as the slit thickness increases and the measured viscosities of 400μm, 500μm and 600μm cavities are almost identical;
- The viscosity curves converge at increasing shear rates.

Dimensionless analysis indicates that heat transfer, including heat convection along the flow direction, surface heat conduction, and viscous heating, have a significant effect on the slit thickness dependent viscosity. The relative wall slip velocity also depends on slit cavity thickness. The competing effects of wall slip and non-isothermal conditions under real molding process conditions serve to determine the slit thickness dependent viscosity. The thermomechanical history induced by the plastication stage (mainly controlled by screw rotation speed, back pressure and dwell time) also has an effect on the rheological behavior of polymer melts in micro injection molding.

This work suggests that wall slip behavior, and non-isothermal conditions should be considered for numerical simulation and process analysis of the micro injection molding process. On-line rheological measurements at the micro/nano meter scale, including plastication stage, can give more precise polymer rheological data than conventional rheology measurements.

Acknowledgments

The authors gratefully acknowledge financial support from Enterprise Ireland (Grant No. CFTD/07/314), the Chinese Scholarship Council, and University College Dublin. We also acknowledge Dr. Jingsong Chu (now at Micromolding Solutions Inc., Canada) for designing the mold and the inserts.

Reference

[1] J.M. Dealy, T.O. Broadhead, Process rheometers for molten plastics: A survey of existing technology, Polymer Engineering & Science, 33 (1993) 1513-1523.

[2] A.L. Kelly, T. Gough, B.R. Whiteside, P.D. Coates, High shear strain rate rheometry of polymer melts, Journal of Applied Polymer Science, 114 (2009) 864-873.

[3] J. Aho, S. Syrjälä, Shear viscosity measurements of polymer melts using injection molding machine with adjustable slit die, Polymer Testing, 30 (2011) 595-601.

[4] P.F. Bariani, M. Salvador, G. Lucchetta, Development of a test method for the rheological characterization of polymers under the injection molding process conditions, Journal of Materials Processing Technology, 191 (2007) 119-122.

[5] G. Gou, P. Xie, W. Yang, Y. Ding, Online measurement of rheological properties of polypropylene based on an injection molding machine to simulate the injection-molding process, Polymer Testing, 30 (2011) 826-832.

[6] A. Pabedinskas, W.R. Cluett, S.T. Balke, Development of an in-line rheometer suitable for reactive extrusion processes, Polymer Engineering & Science, 31 (1991) 365-375.

[7] N. Zhang,C. J. Byrne, D. J. Browne, M.D. Gilchrist, Towards nano-injection molding, Materials Today, In Press (2012).

[8] Y. Donggang, K. Byung, Simulation of the filling process in micro channels for polymeric materials, Journal of Micromechanics and Microengineering, 12 (2002) 604-610.

[9] R.-D. Chien, W.-R. Jong, S.-C. Chen, Study on rheological behavior of polymer melt flowing through micro-channels considering the wall-slip effect, Journal of Micromechanics and Microengineering, 15 (2005) 1389-1396.

[10] J.C. Vasco, J.M. Maia, A.S. Pouzada, Thermo-rheological behaviour of polymer melts in microinjection moulding, Journal of Micromechanics and Microengineering, 19 (2009) 105012.

[11] C.-S. Chen, S.-C. Chen, W.-L. Liaw, R.-D. Chien, Rheological behavior of POM polymer melt flowing through micro-channels, European Polymer Journal, 44 (2008) 1891-1898.

[12] J. Aho, Rheological Characterization of Polymer Melts in Shear and Extension: Measurement Reliability and Data for Practical Processing, PhD thesis, Department of Materials Science, Tampere University of Technology, 2011, p. 54.

[13] H.M. Laun, Polymer melt rheology with a slit die, Rheologica Acta, 22 (1983) 171-185.

[14]K. Walters, Rheometry, Champman and Hall, London, 1975.

[15] R.H.W. P. Schümmer, An elementary method for the evaluation of a flow curve, Chemical Engineering Science, 33 (1978) 759-763.

[16] Y. Chen, D.M. Kalyon, E. Bayramli, Effects of surface roughness and the chemical structure of materials of construction on wall slip behavior of linear low density polyethylene in capillary flow, Journal of Applied Polymer Science, 50 (1993) 1169-1177.

[17] S.G. Hatzikiriakos, J.M. Dealy, Wall slip of molten high density polyethylene. I. Sliding plate rheometer studies, Journal of Rheology, 35 (1991) 497-523.

[18] S.G. Hatzikiriakos, J.M. Dealy, Wall slip of molten high density polyethylenes. II. Capillary rheometer studies, Journal of Rheology, 36 (1992) 703-741.

[19] H. Savvas G, Wall slip of molten polymers, Progress in Polymer Science, 37 (2012) 624-643.

[20] M. Mooney, Explicit formulas for slip and fluidity, Journal of Rheology, 2 (1931) 210-222.

[21] E.E. Rosenbaum, S.G. Hatzikiriakos, Wall slip in the capillary flow of molten polymers subject to viscous heating, AIChE Journal, 43 (1997) 598-608.

[22] C.D. Han, Rheology and Processing of Polymeric Materials: Polymer Rheology, Oxford University Press, New York, 2007.

[23] PEBAX 7233 SN 01, in, CAMPUS http://www.campusplastics.com/campus/en/datasheet/PEBAX+7233+SN+01/ARKEMA/179/75585664.

[24] D. Yao, B. Kim, Scaling issues in miniaturization of injection molded parts, Journal of Manufacturing Science and Engineering, 126 (2004) 733-739.

[25] V. Mhetar, L.A. Archer, Slip in entangled polymer melts. 1. general features, Macromolecules, 31 (1998) 8607-8616.

Table list:

Table 1
Process parameter settings

Cavity thickness (μm)	Material	Injection velocity (mm/s)	Melt temperature (°C)	Mold temperature (°C)	Back pressure (MPa)	Screw rotation speed(rpm)	Dwell time (s)
600	Steel	10	210	120	5	100	5
500	BMG	20					
400	BMG	40					
300	Steel	60					
		80					
		100					
		150					
		200					
		250					
		300					
200	Steel	50					
300	BMG	100					
		150					
		200					
500	BMG	40	200	100	5	50	5
		70	190	80	10	100	15
		100			20	150	30
		150					
		200					

Table 2
Parameters for Carreau-Yasuda model for Pebax 7233

	η_0[MPa s]	λ[s]	a	m
Value	0.00179	0.03329	0.52562	0.50992
Standard error	6.67709E-5	0.01578	0.06714	0.05161

Figure list:

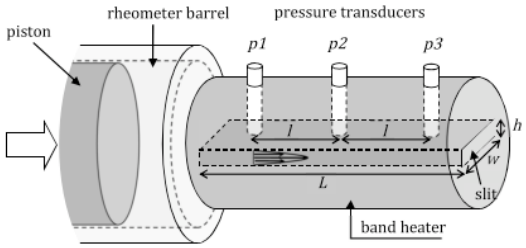

Fig. 1. Schematic of slit rheometer [12].

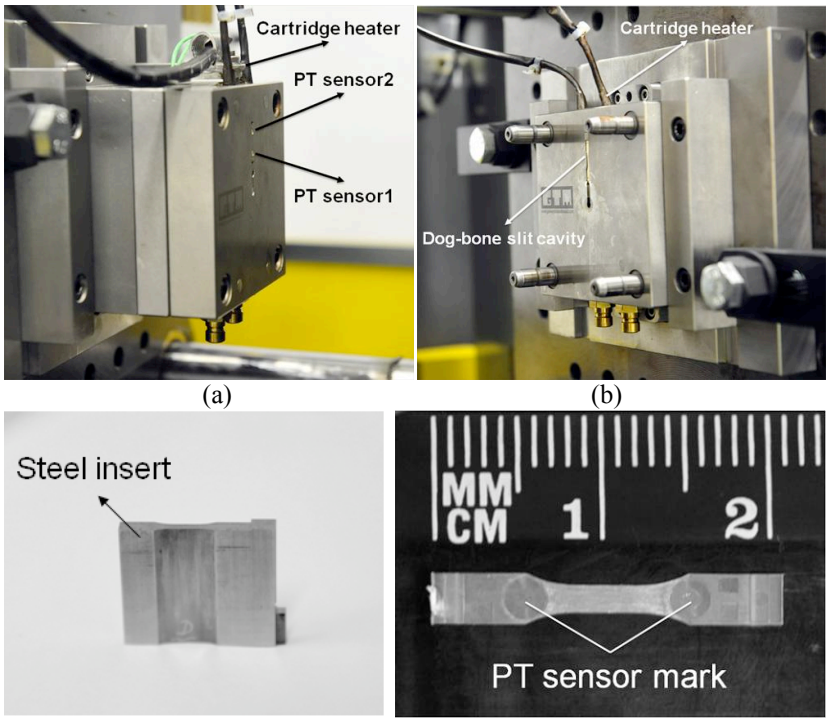

Fig. 2. Mold and measurement system: (a) stationary half, (b) moving half, (c) steel mold insert, (d) molded part.

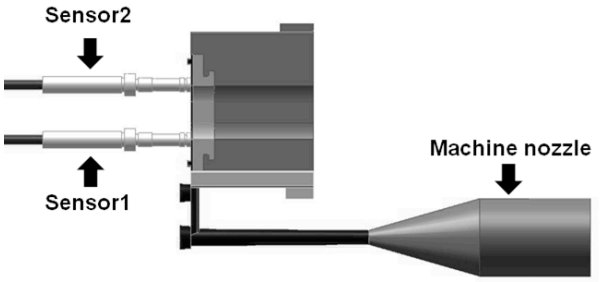

(a)

(b)

Fig. 3. Data acquisition system: (a) PT sensors, (b) CoMo system.

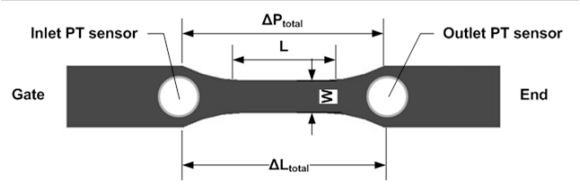

Fig. 4. Locations for PT sensors.

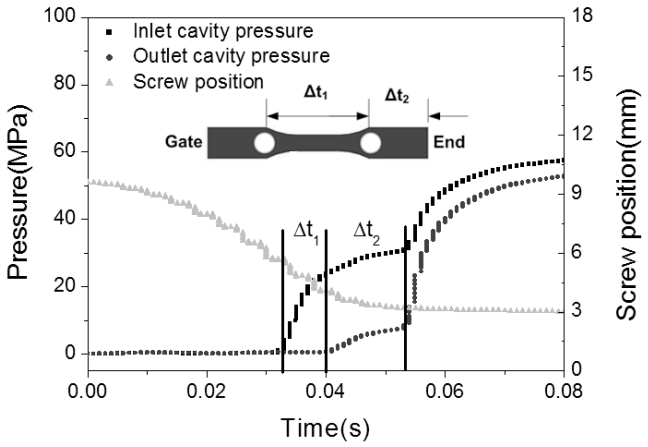

Fig. 5. Typical cavity pressure and injection screw position during flow in the dog-bone die.

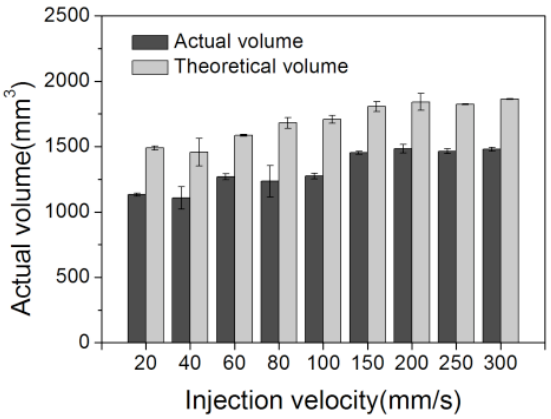

Fig. 6. Comparisons of theoretical injection volume and actual injection volume.

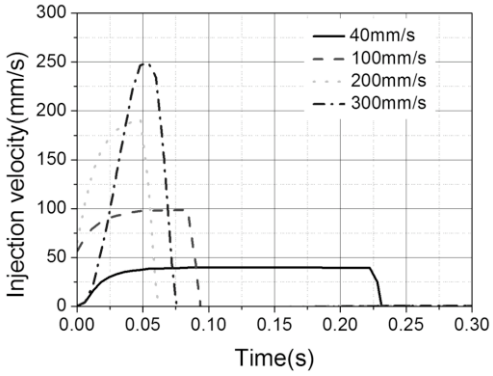

Fig. 7. Profile of injection velocity.

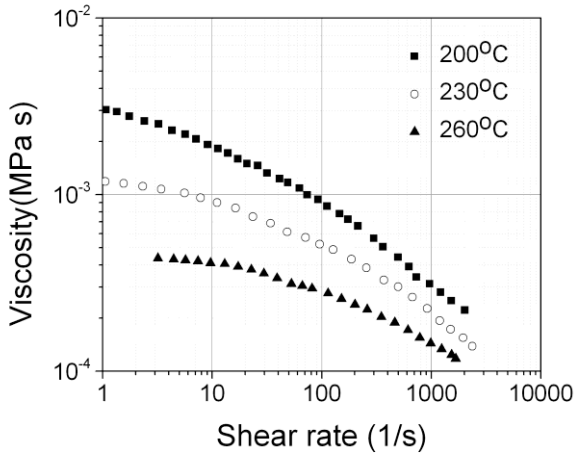

Fig. 8. Viscosity of Pebax 7233.

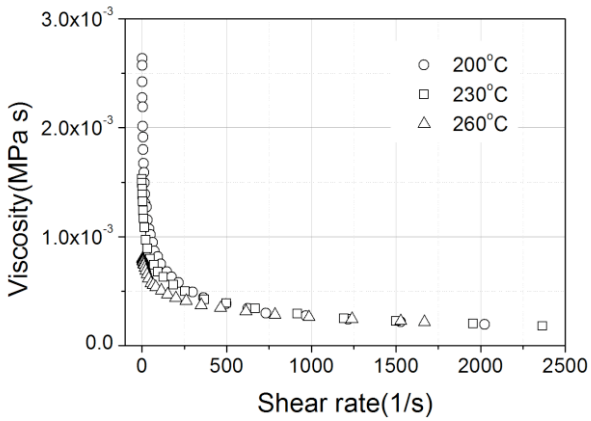

Fig. 9. Master viscosity curves shifted from different temperatures at reference tempreature of 210°C.

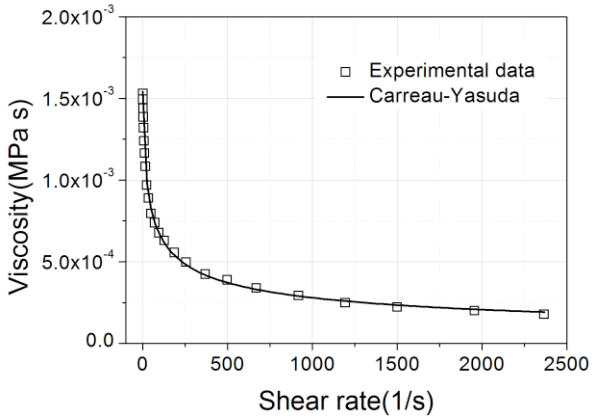

Fig. 10. Master viscosity curves at 210°C.

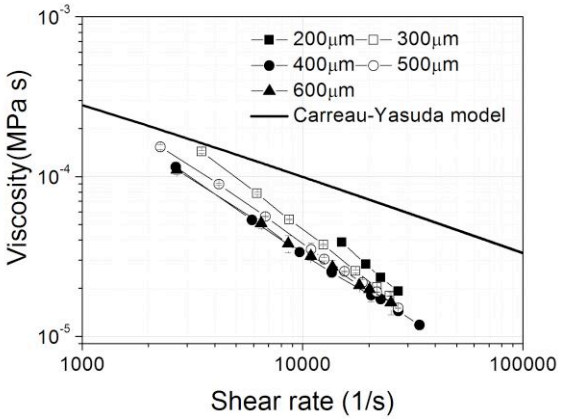

Fig. 11. Measured viscosity and predicted conventional viscosity.

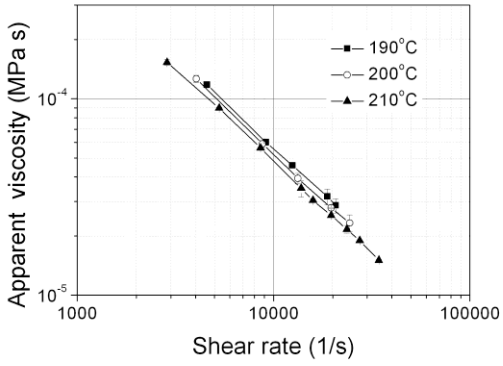

(a)

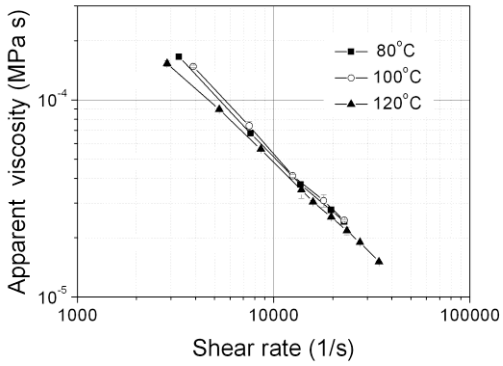

(b)

Fig. 12. Effect of temperature on viscosity: (a) melt temperature, (b) mold temperature.

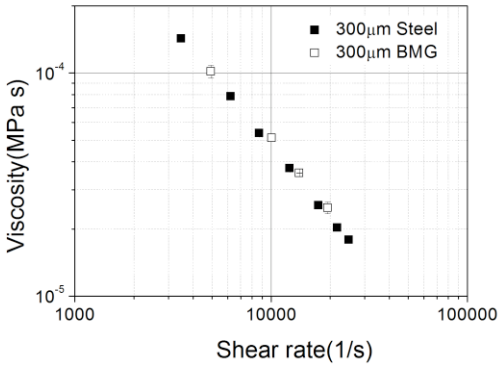

Fig. 13. Comparison of viscosity for different cavity materials

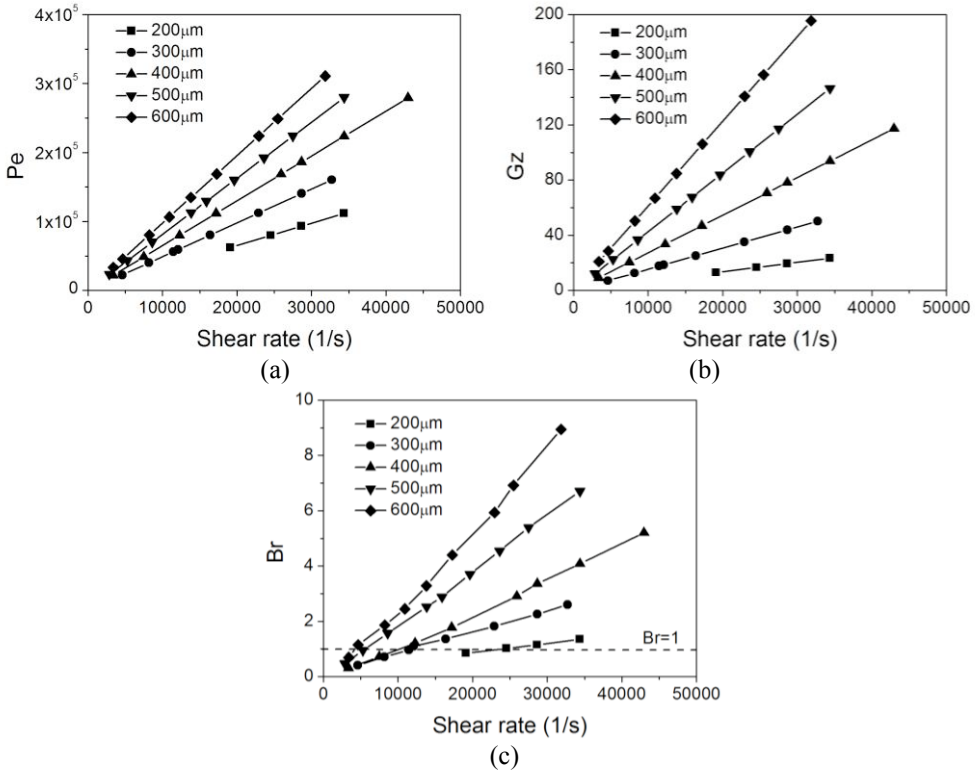

Fig. 14. Effect of cavity thickness and shear rate on dimensionless group: (a) Pe, (b) Gz, (c) Br.

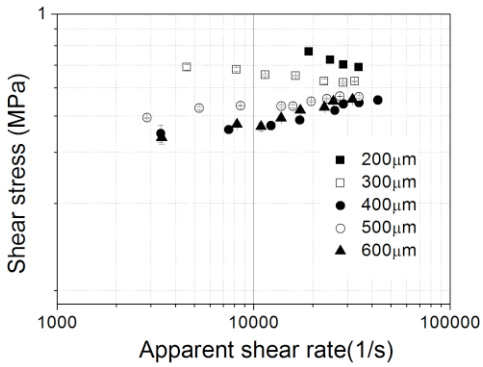

Fig. 15. Flow curves obtained for different cavity thickness.

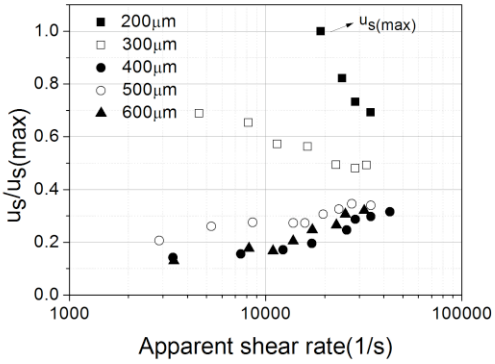

Fig. 16. Relative slip velocity versus shear rate.

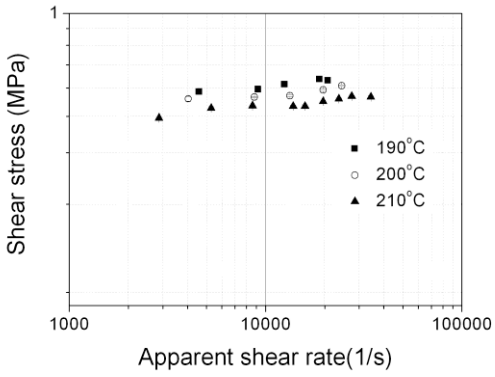

(a)

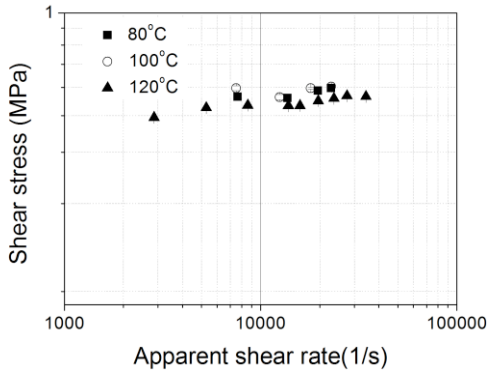

(b)

Fig. 17. Effect of temperature wall shear stress for 500μm channels: (a) melt temperature (b) mold temperature.

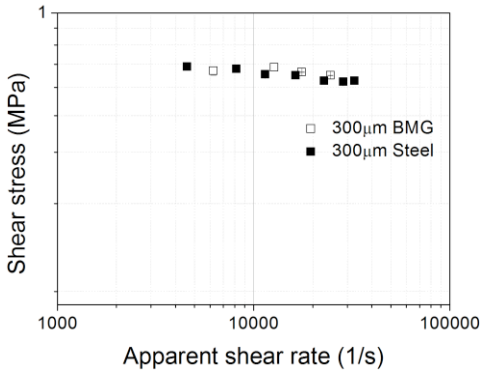

Fig. 18. Effect of roughness and material on wall shear stress (Note Ra of BMG ~30nm and of Steel ~200nm).

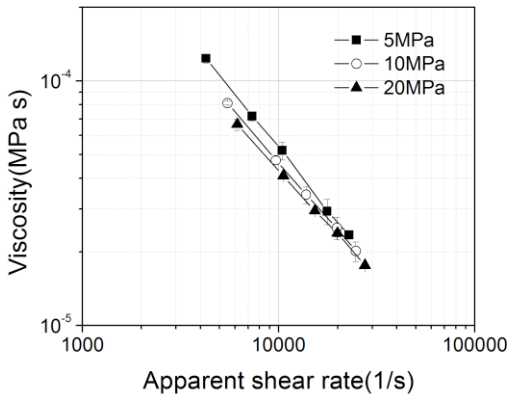

(a)

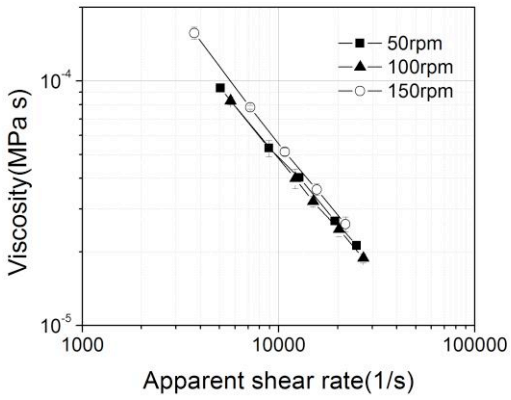

(b)

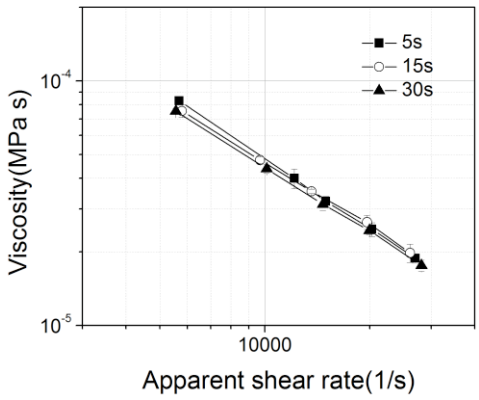

(c)

Fig. 19. Effect of thermomechanical history during plastication on viscosity in the micro injection molding process: (a) back pressure, (b) screw rotation speed, (c) dwell time.